

Performance of a worm algorithm in ϕ^4 theory at finite quartic coupling

Tomasz Korzec, Ingmar Vierhaus and Ulli Wolff*
Institut für Physik, Humboldt Universität
Newtonstr. 15
12489 Berlin, Germany

Abstract

Worm algorithms have been very successful with the simulation of sigma models with fixed length spins which result from scalar field theories in the limit of infinite quartic coupling λ . Here we investigate closer their algorithmic efficiency at finite and even vanishing λ for the one component model in dimensions $D = 2, 3, 4$.

HU-EP-11/03

*e-mail: uwolff@physik.hu-berlin.de

1 Introduction

In reference [1] it was shown how spin systems of the Ising and XY model type can be Monte Carlo simulated with greatly reduced or even eliminated critical slowing down by what the authors call worm algorithms. They can be seen as stochastically sampling strong coupling or hopping parameter expansion graphs of these models to in principle arbitrary order instead of the original spin or field configurations. The method has been generalized in several directions, including sigma models of the $O(N)$ type, and a summary with further references can be found in [2]. All these systems can be regarded as linear¹ sigma or ϕ^4 models, where in the limit of infinite self coupling λ the length fluctuations of the spins are frozen to $N - 1$ dimensional spheres. In this paper it is our goal to systematically investigate for $N = 1$ the dynamical behavior of worm algorithms away from the Ising limit at *finite* λ and even in the Gaussian limit $\lambda = 0$ in Euclidean space dimensions $D = 2, 3, 4$. Results for the Ising limit $\lambda = \infty$ may be inspected for comparison in [3] and [4]. The paper is organized as follows. In Section 2 we discuss the reformulation of ϕ^4 theory and of a few observables by the all-order strong coupling contributions. This is followed by Section 3 detailing our update algorithm and presenting our results on critical slowing down. In Section 4 we summarize our conclusions and in Appendix A we compile data for $\lambda = 1/2$ that can be useful as a reference for future studies. Our report here is a summary of a diploma thesis available under [5] with a lot more details.

2 (Re-)formulation of the model

2.1 Partition function

We use lattice units ($a = 1$) and start from the standard lattice formulation of scalar field theory with the partition function

$$Z_0 = \int \left[\prod_z d\mu_\lambda(\phi(z)) \right] e^{\beta \sum_{l=\langle xy \rangle} \phi(x)\phi(y)} \quad (1)$$

where the measure at each site z is given by

$$\int d\mu_\lambda(\phi) f(\phi) = \frac{\int_{-\infty}^{\infty} d\phi e^{-\phi^2 - \lambda(\phi^2 - 1)^2} f(\phi)}{\int_{-\infty}^{\infty} d\phi e^{-\phi^2 - \lambda(\phi^2 - 1)^2}} \quad (2)$$

and thus includes the coupling $\lambda \geq 0$. Our hypercubic lattice is wrapped on a D dimensional torus with L sites in each direction, and the sum is over links l

¹Spins live in the linear space \mathbb{R}^N but, of course, are still nonlinearly coupled in general.

corresponding to nearest neighbor pairs of sites $\langle xy \rangle$. Below we shall need the moments

$$c_\lambda(n) = \int d\mu_\lambda(\phi) \phi^n. \quad (3)$$

In particular for the λ values simulated in this study the nonvanishing even moments are

$$c_0(2n) = \Gamma(n + 1/2)/\Gamma(1/2) = 2^{-n}(2n - 1)!!, \quad (4)$$

$$c_{1/2}(2n) = 2^{n/2}\Gamma(n/2 + 1/4)/\Gamma(1/4), \quad (5)$$

$$c_\infty(2n) = 1, \quad (6)$$

while odd moments vanish due to $Z(2)$ symmetry.

The fundamental two point correlation function is regarded as a ratio

$$G(u - v) = \langle \phi(u)\phi(v) \rangle = \frac{Z(u, v)}{Z_0} \quad (7)$$

with the ‘partition function with insertions’ as numerator

$$Z(u, v) = \int \left[\prod_z d\mu_\lambda(\phi(z)) \right] e^{\beta \sum_{l=\langle xy \rangle} \phi(x)\phi(y)} \phi(u)\phi(v). \quad (8)$$

By expanding in β the Boltzmann factor on each link and then integrating over ϕ independently on each site using (3) the same quantity is given by

$$Z(u, v) = \sum_k \left[\prod_l \frac{\beta^{k(l)}}{k(l)!} \right] \prod_x c_\lambda(\partial k(x) + \delta_{x,u} + \delta_{x,v}). \quad (9)$$

Here the sum is over a link field that is independently summed over $k(l) = 0, 1, \dots, \infty$ and the divergence

$$\partial k(x) = \sum_{l, \partial l \ni x} k(l) \quad (10)$$

counts the sum of $k(l)$ over all links surrounding a site x . We have a well defined non-negative weight for any k configuration. Nonzero contributions arise if ∂k is even everywhere except the sites u, v if they do not coincide, where ∂k must be odd. Finally we introduce the ensemble²

$$\mathcal{Z} = \sum_{u,v} Z(u, v) = \sum_{k,u,v} \left[\prod_l \frac{\beta^{k(l)}}{k(l)!} \right] \prod_x c_\lambda(\partial k(x) + \delta_{x,u} + \delta_{x,v}) \quad (11)$$

²A weight depending on the locations u, v could be included as in [4], but we have not yet explored this generalization.

which will be simulated by the worm algorithm. In this way expectation values

$$\langle\langle\mathcal{O}[k; u, v]\rangle\rangle = \frac{1}{\mathcal{Z}} \sum_{k,u,v} \left[\prod_l \frac{\beta^{k(l)}}{k(l)!} \right] \left[\prod_x c_\lambda(\partial k(x) + \delta_{x,u} + \delta_{x,v}) \right] \mathcal{O}[k; u, v] \quad (12)$$

become accessible to Monte Carlo estimation.

2.2 Observables

The fundamental two point function is now given by

$$G(x) = \langle\phi(x)\phi(0)\rangle = \frac{\langle\langle\delta_{x,u-v}\rangle\rangle}{\langle\langle\delta_{u,v}r_\lambda(\partial k(u))\rangle\rangle} \quad (13)$$

where we have introduced

$$r_\lambda(2n) = \frac{c_\lambda(2n)}{c_\lambda(2n+2)}, \quad (14)$$

which is only required and defined for even arguments. For universal quantities only ratios of two point functions at differing separations are of interest and then the denominator is not required. It is however related to the susceptibility

$$\chi = \sum_x G(x), \quad \chi^{-1} = \langle\langle\delta_{u,v}r_\lambda(\partial k(u))\rangle\rangle. \quad (15)$$

The second moment (renormalized) mass m can be defined and then measured by

$$\frac{\sum_x \cos(2\pi x_\mu/L) G(x)}{\chi} = \frac{m^2}{m^2 + 4 \sin^2(\pi/L)} = \langle\langle f_m(u-v) \rangle\rangle \Rightarrow m \quad (16)$$

with

$$f_m(x) = \frac{1}{D} \sum_\mu \cos(2\pi x_\mu/L). \quad (17)$$

Note that in our symmetric setup each of the D directions contributes equally and we average for better statistics.

An estimator for the energy (without the measure part) is given by

$$E = \frac{1}{DL^D} \frac{\partial}{\partial \beta} \ln Z_0 = \frac{1}{\beta DL^D} \frac{\langle\langle\delta_{u,v}r_\lambda(\partial k(u)) \sum_l k(l)\rangle\rangle}{\langle\langle\delta_{u,v}r_\lambda(\partial k(u))\rangle\rangle}. \quad (18)$$

A second estimator for E is given by the nearest neighbor correlation using (13). As in the Ising limit [4] the error is much larger in this case.

3 Algorithm and dynamical results

In the first Subsection we describe details of the worm algorithm implemented by us. The code was written in C and has run on standard dual quad-core PCs. The data reported below correspond to a few core-months total runtime dominated by the largest lattices of sizes 128^3 and 32^4 .

3.1 Specification of the update scheme

The update algorithm used by us is a generalization of the one described in [4]. We define two types of micro-steps that each obey detailed balance with respect to the ensemble (11):

- *I*: With equal probability we pick one of the $2D$ neighbors u' of the present configuration's u and denote by l the link in between. Again with equal probability we propose one of the two moves $k(l) \rightarrow k(l) \pm 1$ accompanied in either case by the change $u \rightarrow u'$. The proposal is accepted with the respective Metropolis probabilities $\min(1, q_{I\pm})$ where we take

$$q_{I+} = \frac{\beta}{k(l) + 1} r_\lambda^{-1} (\partial k(u') + \delta_{u',v}) \quad (19)$$

and

$$q_{I-} = \frac{k(l)}{\beta} r_\lambda (\partial k(u) + \delta_{u,v} - 1). \quad (20)$$

- *II*: We only act if $u = v$ holds, and even then only with probability $p_0 = 1/2$. Then a randomly chosen new location $u' = v'$ (at unchanged k) is proposed and accepted with probability $\min(1, q_{II})$,

$$q_{II} = \frac{r_\lambda(\partial k(u))}{r_\lambda(\partial k(u'))}. \quad (21)$$

Swapping the rôles of u and v , step *I* can also be applied to move v and we call these possibilities now I_u and I_v . As an iteration we define the $L^D/2$ fold repetition of the sequence $I_u II I_v II$ which is similar to a sweep of a standard local algorithm as far as CPU work is concerned.

3.2 Monte Carlo dynamics in the Gaussian limit

For the Gaussian case $\lambda = 0$ all our observables can be computed exactly by straight forward Fourier expansion. We therefore do not list any mean values in this case but we have monitored that our results were correct within errors. The

dynamics of the ‘worm’ algorithm remains of interest at $\lambda = 0$ and is presumably representative for other small bare couplings. To investigate critical slowing down we keep constant the extension in physical units mL while we increase L . In the free case this leads to choosing

$$\beta^{-1} = D + \frac{m^2}{2}. \quad (22)$$

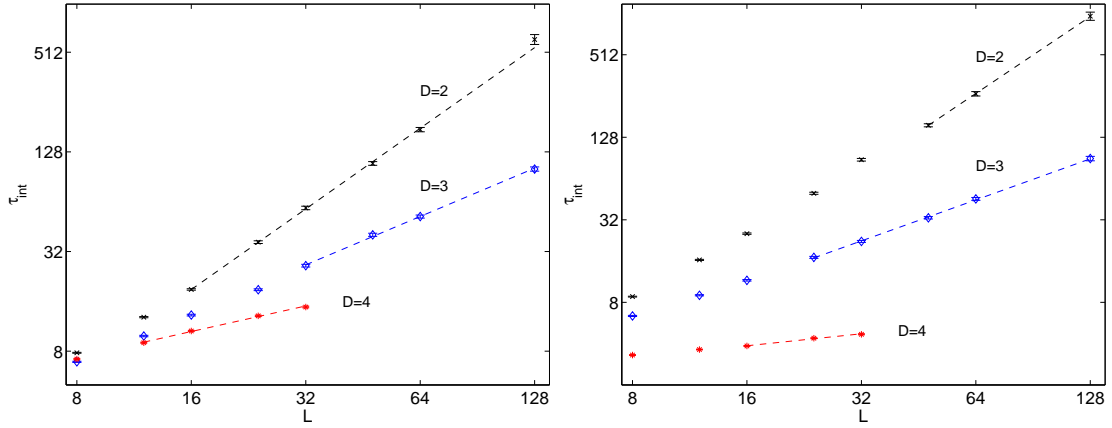


Figure 1: Integrated autocorrelation times for the energy E (left panel) and the mass m (right panel) for the Gaussian model in dimensions $D = 2, 3, 4$ with $mL = 4$. The dashed lines are fits of the form $\tau_{\text{int}} \propto L^z$, z -values are in the text.

All autocorrelation times were determined as discussed in [6] and are given in units of ‘iterations’ defined above. Measurements are taken and pre-averaged during each iteration and then stored for off-line analysis. In Fig. 1 we see log-log plots of integrated autocorrelation times for the observables E and m . Note that the estimator (18) refers to a ratio of primary Monte Carlo estimated mean values and we refer to [6] for the definition of τ_{int} for such derived quantities. The dashed lines are fits with dynamical exponents z . From top to bottom we have determined $z = 1.62(2), 0.97(3), 0.51(2)$ (left plot) and $z = 1.86(7), 0.99(2), 0.29(2)$ (right plot). The quoted errors are purely statistical. We consider these fits which have acceptable χ^2 over the range shown as mere parameterizations of our data in the range where most simulations work. We have not embarked on the difficult assessment of systematic errors with regard to truly asymptotic dynamical behavior. In summary we see here distinct critical slowing down, weaker than for standard local methods but inferior to worm (and also cluster) simulations in the Ising limit. There is a pronounced tendency of decorrelation improving

with increasing dimension. The susceptibility χ was also investigated and behaves similarly to m . The ultraviolet quantity $G(0)$ measured via (13) on the other hand typically exhibits shorter autocorrelations. We also have a large set of data in smaller volumes $mL = 1$. Autocorrelations are larger for this more critical series but the overall qualitative behavior is quite similar. Further details can be found in [5].

3.3 Monte Carlo dynamics at intermediate coupling

We now turn to simulations at $\lambda = 1/2$ which are otherwise organized similarly to those of the previous subsection. As the values of our observables are non-trivial we collect them in Appendix A for this case. The dynamical results are given in Fig. 2.

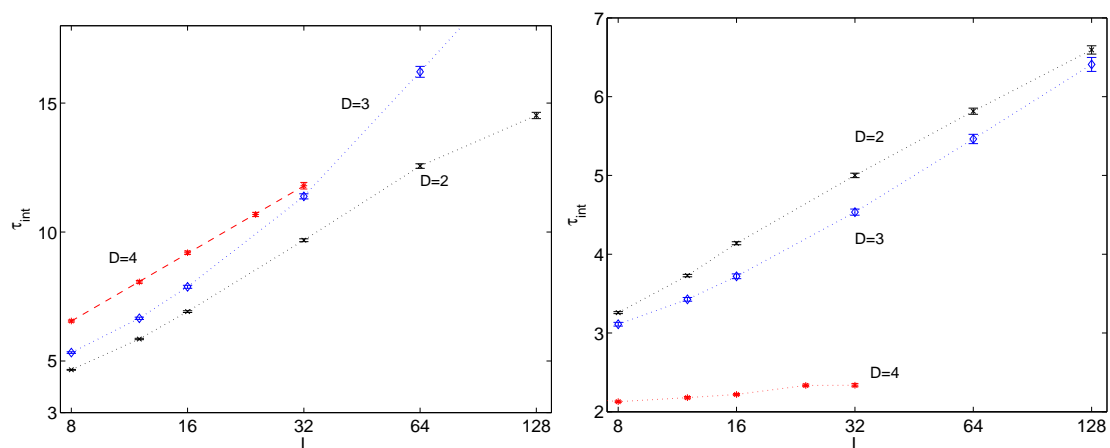


Figure 2: Integrated autocorrelation times for energy E (left panel) and mass m (right panel) for $\lambda = 1/2$ in dimensions $D = 2, 3, 4$ with $mL = 4$. The dashed line is a fit for τ_{int} linear in $\ln L$, while the dotted lines just connect data points to guide the eye.

We have chosen semilogarithmic plots as the most natural appearing common format here. Two term fits linear in $\ln L$ do however not quite achieve good χ^2 values except for E in $D = 4$ (dashed line). What is clearly visible is that the worm algorithm works much better in this interacting case than in the Gaussian limit. Although precise fits require more than the first power of $\ln L$ (or larger L to assume the asymptotic form) the general behavior looks close to an only logarithmic growth of autocorrelations. The tendency with D is mild and the ordering differs for the two observables displayed. Also at this coupling we have

looked at further observables and have also simulated $mL = 1$ with qualitatively similar outcomes.

4 Conclusions

We have found that a worm algorithm is applicable to ϕ^4 theory all the way to the Gaussian limit in dimensions between two and four. Although still exhibiting less critical slowing down than standard local methods, the free limit $\lambda = 0$ is the most difficult case for the worm algorithm. For the intermediate coupling $\lambda = 1/2$ the situation is already similar to the infinite coupling limit with regard to decorrelation. While at zero coupling the efficiency shows pronounced improvement with growing dimension, this dependence is much weaker at $\lambda = 1/2$. In [7] a very dramatic improvement was realized in the Ising limit by the construction of a special estimator for the connected four point function without the need to perform numerical cancellations. We have so-far not succeeded in generalizing this construction to finite λ in a similarly efficient way. Some such efforts are however reported in [5].

Acknowledgments. We thank Martin Hasenbusch for discussions. Financial support of the DFG via SFB transregio 9 is acknowledged.

A Results of simulations at $\lambda = 1/2$

In this appendix we report on some mean values of observables defined in (16), (18), (15) together with β values that have been determined by tuning to $mL = 4$ within errors. The data are summarized in tables 1, 2, 3. The last column holds the numbers of iterations performed. We note that the mass m has a practically constant and mostly sub per mille error at – or rescaled to – a constant iteration number. This confirms the very mild or even absent slowing down.

L	β	mL	E	χ	its/ 10^6
8	0.576950	4.0036(20)	0.26184(13)	6.566(5)	24
12	0.615670	3.9982(22)	0.32214(13)	13.381(11)	24
16	0.634350	4.0008(23)	0.36241(12)	22.274(20)	24
22	0.649270	4.0028(25)	0.40381(11)	39.334(38)	24
32	0.661390	3.9991(26)	0.44622(9)	76.855(80)	24
64	0.674330	4.0067(29)	0.50603(7)	262.87(30)	24
128	0.680679	3.9936(35)	0.54516(5)	898.3(1.2)	20

Table 1: Results at $D = 2$.

L	β	mL	E	χ	its/ 10^6
8	0.370240	3.9994(26)	0.14561(7)	10.610(12)	8
12	0.383030	3.9984(27)	0.16235(5)	22.915(28)	8
16	0.388310	3.9957(28)	0.17178(4)	39.963(50)	8
22	0.391920	4.0007(29)	0.17989(3)	74.06(10)	8
32	0.394390	3.9999(30)	0.18692(2)	154.08(21)	8
64	0.396400	3.9998(32)	0.19457(1)	600.02(90)	8
128	0.397067	4.0059(49)	0.19816(1)	2336.9(5.3)	4

Table 2: Results at $D = 3$.

L	β	mL	E	χ	its/ 10^6
4	0.245490	4.0021(20)	0.079119(52)	4.0522(34)	8
8	0.271670	4.0012(17)	0.092157(16)	14.624(14)	8
12	0.277630	3.9977(15)	0.097502(8)	32.183(23)	8
16	0.279870	4.0003(15)	0.099984(5)	56.669(39)	8
24	0.281560	3.9972(14)	0.102197(3)	126.869(83)	8
32	0.282173	4.0007(19)	0.103132(4)	224.41(20)	4

Table 3: Results at $D = 4$.

References

- [1] N. Prokof'ev and B. Svistunov, *Worm Algorithms for Classical Statistical Models*, *Phys. Rev. Lett.* **87** (2001) 160601.
- [2] U. Wolff, *Strong coupling expansion Monte Carlo*, Contribution to the proceedings of Lattice 2010, Sardinia, Italy.
- [3] Y. Deng, T. M. Garoni, and A. D. Sokal, *Dynamic Critical Behavior of the Worm Algorithm for the Ising Model*, *Phys. Rev. Lett.* **99** (2007) 110601.
- [4] U. Wolff, *Simulating the All-Order Strong Coupling Expansion I: Ising Model Demo*, *Nucl. Phys.* **B810** (2009) 491.
- [5] I. Vierhaus, *Simulation of ϕ^4 Theory in the Strong Coupling Expansion beyond the Ising Limit*, Diploma Thesis, Humboldt University, 2010, <http://nbn-resolving.de/urn:nbn:de:kobv:11-100180119>

- [6] ALPHA Collaboration, U. Wolff, *Monte Carlo Errors with less Errors*, *Comput. Phys. Commun.* **156** (2004) 143.
- [7] U. Wolff, *Precision check on triviality of ϕ^4 theory by a new simulation method*, *Phys. Rev.* **D79** (2009) 105002.